Hindawi
Advances in Civil Engineering
Volume 2019, Article ID 4528230, 11 pages
https://doi.org/10.1155/2019/4528230

Research Article

An Improved Low-Cost Continuous Compaction Detection Method for the Construction of Asphalt Pavement

Tong Jia, Tiejun He, Zhendong Qian, Jian Lv, and Kaixin Cao

Intelligent Transportation System Research Center, Southeast University, Nanjing 211189, China

Correspondence should be addressed to Tiejun He; hetiejun@seu.edu.cn

Received 25 January 2019; Revised 17 May 2019; Accepted 3 June 2019; Published 26 June 2019

Academic Editor: Hui Yao

To realize the continuous compaction control (CCC) of asphalt pavement during construction, continuous detection method was investigated for the compaction degree values. For the trajectory of rollers, a collaborative positioning method was proposed. For the monitoring of rolling process, an embedded-based detection system was designed. For the evaluation of rolling effect, harmonic analysis was introduced and a new index, vibration compaction energy value (VCV_e), was proposed. Positioning experiments were conducted, and the accuracy was improved to 0.48 m. Rolling tests were performed, and typical compaction meter values (CMVs), compaction control values (CCVs), and VCV_e were obtained. The referenced compaction degree by conventional way was 94.6%, which was used to calibrate the detected values of compaction degree indexes. The results showed that continuous compaction detection can be achieved based on positioning system and vibration analysis. Compared with CMV and CCV, VCV_e is less discrete, more stable, and consistent to describe the compaction state. Though, all the CMV, CCV, and VCV_e indexes are unable to be used for quality assurance directly or alone, they could be an aid for quality control. Continuous compaction detection system meets the monitoring requirements of pavement construction at a lower cost and could lay a foundation for the intelligent compaction (IC).

1. Introduction

During the construction of asphalt pavement, rolling is one of the most important processes for road performance and project quality. Substandard compaction may lead to deterioration and affect traffic operations, resulting in economic losses [1, 2]. The compaction degree is a key indicator of construction quality, and the detection methods are usually divided into traditional ways, online ways, and continuous ways. The traditional ways include the cutting ring sampler method, sand filling method, core cutter method, nuclear method, and so on. These methods are simple and easy to conduct; however, most of them are postdetection modes and difficult to describe the compaction conditions in real time. In addition, some traditional methods may cause damage to the pavements [3–5]. The online methods make up for the shortcomings of traditional ways and detect the compaction degree nondestructively, typically including the Rayleigh wave method, nonnuclear density method, falling weight deflectometer (FWD) method, etc [6–8]. Nevertheless, all of them are pointing-detection and result control methods, which are difficult to realize the process control [9]. In comparison, the continuous compaction detection methods could obtain comprehensive information of the rolling process continuously [10]. By adjusting operations through feedback mechanism in real time, the continuous ways attract attentions in different construction areas all over the world gradually [11–16].

The research of continuous compaction detection was originated from Europe in early 1970s. Based on the dynamic relationship between filling materials and vibrating roller wheels [17, 18], Thurner proposed the harmonic analysis method in the study of subgrade soil compaction and evaluated the rolling effects of pavement materials by analyzing the frequency components of vibration signals [19]. Dynapac and Geodynamik developed an index, compaction meter value (CMV), to reflect the compaction degree together, applied to the compaction of fine-grained soil and stone materials [20]. On this basis, for the needs of soil compaction, as well as the compaction of earth and stone mixtures, researchers have successively introduced indexes such as compaction control value (CCV), total harmonic distortion (THD), etc [21, 22]. Entering the twentieth century, some roller manufacturers introduced mechanical indexes to describe the compaction conditions, such as machine drive power (MDP) of Caterpillar, vibration modulus E_{vib} of BOMAG, etc [23, 24]. However, most of them can only be used with specific rolling machines, and the suitable filling materials are relatively less, which limit the application range [25]. In China, Xu et al. advocated the continuous compaction control method which focused on the compaction detection of gravel roadbed from 1993 and applied to the monitoring system of base construction for high-speed railway in recent years [26].

Due to the development history of road engineering and railway engineering, previous studies on continuous compaction detection are mainly focused on the compaction of subgrade soil and earth-rock mixtures [27]. Although the geotechnical compactions can be used as references for the compaction of asphalt pavement, there are still great differences because of the structural and performance requirements [28, 29]. From 2004, the Federal Highway Administration (FHWA), a USDOT agency, supported the "Intelligent Compaction Research Program" [30]. With the application of computer system, vehicle sensors, positioning system, and monitoring software, compaction detection systems were researched for the compaction of soil and asphalt mixture, and relevant specifications were developed. In the construction equipment market, there are typical products such as AccuGrade system of Caterpillar, Vario-Control system of BOMAG, etc [31, 32]. In China, there are a few cases of continuous compaction detection on asphalt pavement. For example, Zhang analyzed the relationship between the measured CMV data and traditional detection indexes. The results showed that the correlation was weak, and the CMV index cannot be used for quality assurance alone [33].

In summary, the compaction state of pavement materials can be obtained by analyzing the time-frequency characteristics of responsive vibration signals in real time [34]. Based on the signal analysis and operation adjustment, the construction quality could be controlled timely [35, 36]. Therefore, it is important to research the continuous compaction detection method for the nondestructive monitoring and feedback control [37]. However, the current compaction control systems usually choose industrial computer to realize system control and data calculation and make use of high-precision positioning technology to obtain information such as rolling position. In consequence, the high costs of such systems may limit their promotion in developing areas. For example, China is in the era of infrastructure construction, and there is a great need for continuous compaction control (CCC) system, but the applications of CCC are still less. Therefore, continuous compaction detection technology was studied in this paper. To improve the accuracy and continuity of compaction detection in real time while reducing the costs, an embedded-based detection system was developed, as well as a collaborative positioning system.

2. Methodology

2.1. Collaborative Positioning Theory. Since the numbers of rolling passes affect compaction quality directly, the CCC system needs to match the compaction degree values to the corresponding rolling positions. Thus, a high-precise positioning of the rollers is in great need. A collaborative positioning system was developed as shown in Figure 1, and the Global Positioning System (GPS) was used to track the rollers for number of passes and extract velocity and azimuth data at the same time. The ultra wideband (UWB) system was used to obtain the real-time positions of the rollers.

According to the basic propagation principles of electromagnetic wave, the spatial coordinates of GPS receiver (x, y, z) can be determined based on the distances between satellites and receiver, combining with the current satellite positions (x_i, y_i, z_i).

For the UWB system, according to the scene of pavement construction, two-dimensional Cartesian coordinate system can be established. Based on Figure 1, the points A, B, and C are set as centres where the three base stations are placed, and d_a, d_b, and d_c, the distances between tag and base stations, are set as radii to draw three circles separately. The circles will intersect each other at the point O, where the mobile tag is located. If the coordinates of points A, B, and C are known as (x_a, y_a), (x_b, y_b), and (x_c, y_c), the coordinate of intersection point O is set as (x, y). According to the distance geometry theory, the distances between point O and points A, B, and C could be obtained.

$$\begin{cases} (x-x_a)^2 + (y-y_a)^2 = d_a^2, \\ (x-x_b)^2 + (y-y_b)^2 = d_b^2, \\ (x-x_c)^2 + (y-y_c)^2 = d_c^2. \end{cases} \tag{1}$$

In addition, the value of each radius can be obtained through the two-way time of flight (TW-TOF) ranging algorithm by UWB tags. Based on the trilateration positioning algorithm and three-sphere intersection positioning principle, the coordinate of point O will be determined [38].

$$\begin{aligned} \begin{bmatrix} x \\ y \end{bmatrix} = {}& \begin{bmatrix} 2(x_a-x_c) & 2(y_a-y_c) \\ 2(x_b-x_c) & 2(y_b-y_c) \end{bmatrix}^{-1} \\ & \cdot \begin{bmatrix} x_a^2 - x_c^2 + y_a^2 - y_c^2 + d_c^2 - d_a^2 \\ x_a^2 - x_c^2 + x_b^2 - x_c^2 + d_c^2 - d_b^2 \end{bmatrix}. \end{aligned} \tag{2}$$

The speed and azimuth data collected by GPS system and (x, y) obtained by UWB system are measurement information. Finally, the accuracy was improved with extended Kalman filter algorithm [39, 40].

2.2. Compaction Degree Acquisition. Vibration signals were obtained by the detection system, and harmonic analysis was conducted. Thereby, compacting information will be

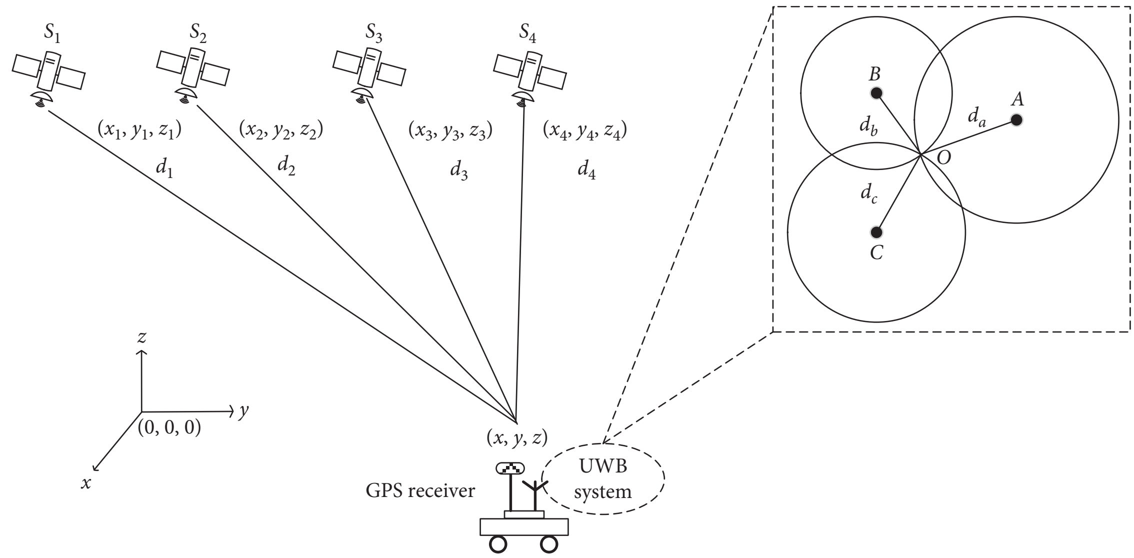

Figure 1: GPS/UWB collaborative positioning schematic.

extracted, and then the relationships between compaction degree and numbers of passes could be concluded [41].

2.2.1. Harmonic Analysis Method. Harmonic analysis is a branch of mathematics concerned with the representation of signals as the superposition of basic waves and the notions of Fourier series and Fourier transforms (i.e., an extended form of Fourier analysis). In the past two centuries, it has become a vast subject with applications in areas as diverse as number theory, representation theory, signal processing, quantum mechanics, tidal analysis, and neuroscience. Based on the Fourier analysis, any complex wave can be composed of many sinusoidal components with different frequencies, amplitudes, and phases. Therefore, harmonic analysis can be used to determine the nonlinear distortion [42].

To obtain the spectral characteristics for harmonic analysis, the time-frequency domain conversion of vibration signals is needed. In view of the real-time detection and hardware utilization, fast Fourier transform (FFT) algorithm was applied [43].

Let the sampling frequency be f_s and the sampling points number be N. The results of FFT algorithm are N complex values, which reflect the characteristics of frequency-domain signals. The frequency corresponding to the nth point is f_n.

$$f_n = \frac{(n-1)f_s}{N}, \quad n = 1, 2, \ldots, N. \tag{3}$$

In equation (3), if $n = 1$, the frequency f_0 is 0 Hz. In fact, the complex value corresponding to f_0 represents the direct current (DC) component of original vibration signal, which is independent of roller vibration and should be eliminated before the harmonic analysis. If $n \geq 2$, the modulus of complex values are amplitudes of vibration signals at the corresponding frequencies. Thereby, the amplitudes of the fundamental wave and each harmonic wave could be extracted.

2.2.2. Compaction Degree Indexes. As the rolling process is going, the compactness of filling materials increases gradually, and the responsive vibrating acceleration signals change gradually as well. The vibration signals contain fundamental wave components, harmonic wave components, and some other clutter interferences. Based on the harmonic analysis, the amplitude ratios between harmonics and fundamental frequency reflect the distortion of vibration signals. Furthermore, the variation can be used to describe the compaction states of filling materials [44]. Among the compaction degree indexes based on harmonic analysis, CMV and CCV are most widely used, and the harmonic components are easy to extract, with definitions given in equations (4) and (5) [45].

$$\mathrm{CMV} = \mathrm{Cal} \cdot \frac{A_{2\Omega}}{A_{\Omega}}, \tag{4}$$

$$\mathrm{CCV} = \mathrm{Cal} \cdot \left[\frac{A_{0.5\Omega} + A_{1.5\Omega} + A_{2.5\Omega} + A_{3\Omega}}{A_{0.5\Omega} + A_{\Omega}}\right]. \tag{5}$$

In Equation (4), $A_{2\Omega}$ and A_{Ω} are amplitudes of the second harmonic and fundamental waves decomposed from acceleration signals, respectively. Cal is the calibration coefficient which needs to be calibrated in practice and usually set as 300 initially. Comparing with CMV, CCV in equation (5) considers half frequencies within the third harmonic frequency, and Cal is usually set as 100 initially.

In practical applications, it is found that the compactness states of filling materials during rolling process are mainly affected by the work of rollers. However, since the constitutive relationship of filling materials is nonlinear, there are also some other frequency signals generated in addition to the original multiple frequency and half frequency signals. According to the signal and system theory and the convergence of spectrum, the power spectrums of signal are mainly concentrated at the low frequency band. Also, according to Parseval's energy conservation theorem, the energy sum of the components in time-domain is equal to the energy sum in frequency-domain. Therefore, based on the existing indexes, a new index VCV_e was proposed and defined as follows:

$$\begin{gathered}VCV_e = \mathrm{Cal}\cdot\frac{\sum_{i=1}^{N}A_{\Omega_i}}{A_{\Omega}^2},\\ A_{\Omega_i}\leq A_{\Omega_{i-1}},\frac{A_{\Omega_i}^2}{A_{\Omega}^2+\sum_{i=1}^{N}A_{\Omega_i}^2}\leq\alpha, i=1,2,\ldots,N.\end{gathered} \tag{6}$$

In equation (6), the threshold ratio α is usually set as 5% initially and the calibration coefficient Cal is usually set as 100 initially. Thereby, the interference and noise can be reduced effectively. Based on the perspective of energy distribution, VCV_e considers the frequency components generated by various nonlinear effects and finally limits the deviation of existing indexes. In the end, the compaction degree values can be calculated based on equations (4)–(6).

3. Implementation of the Detection System

For the CCC systems of asphalt pavement, there are seven primary manufacturers in the world. Specifically, these manufacturers include Case-Ammann, BOMAG, Caterpillar, Dynapac, Hamm-Wirtgen, Volvo and Sakai, and their typical products are shown in Table 1.

Based on Table 1, a typical CCC system usually consists of a positioning unit, a control unit, and several measurement sensors. According to the FHWA report [46], a CCC roller may cost 3%–5% more than a conventional roller (In China, the price of a 12t roller is usually around \$40,000~\$60,000), and retrofitting an existing roller with IC equipment can see costs ranging from \$50,000–\$75,000. In addition, taking Trimble GPS product as an example, it costs \$1,800 around per year for positioning resource rental.

Moreover, although the CCC system products listed in Table 1 possess many advantages, managers and technical staff in developing areas have to consider the costs. Thus, the promotion of CCC systems is limited. Given this, we are attempting to find approaches to achieve similar performance with less cost. However, for the sensors of measuring vibration, temperature, and angle, the cost is almost fixed since they are standard industrial products. Despite this, these sensors account for a small proportion of total cost by comparing with other units. Therefore, to reduce the overall cost, we emphasized on the positioning unit and control unit and designed an embedded-based continuous compaction detection system with the structure shown as Figure 2. The cost of designed system is estimated to be around \$2,500 with "all the bells and whistles" (civil GPS module (\$200), touch screen tablet (\$600), embedded device (\$500), and measurement sensors (\$800)). In addition, there is no resource rental fee for the use of civil GPS module.

Based on Figure 2, the detection system consists of signal acquisition unit, processor unit, positioning system unit, and so on. Including acceleration sensor and constant current source circuit, the signal acquisition unit is the front-end to detect vibration signals for the compaction information. Considering the advantages of small size, large range, and high precision, the accelerometer sensor selected CT1010 L module of Chengke, which meets the specific detection requirements of roller vibration.

For the positioning system unit, the civilian GPS module chosen was NEO-6M module of Waveshare for its low cost, although the accuracy is usually larger than 2.5 m. Similarly, considering the lower power consumption, with accuracy of less than 0.1 m, the UWB system selected DW1000 module of Decawave, but the range is limited by communication distance of tags.

Dual-processor architecture was proposed to cover the needs of system control and signal processing, as well as the utilization efficiency of hardware resources. Taking advantages of lower power consumption and good scalability, the main processor selected was i.MX6Q module of Freescale to realize data transmission and process control. The coprocessor chosen was STM32F4 module of STMicroelectronics to complete sampling and signal processing for fast signal acquisition. In addition, a human-computer interaction (HCI) based on Qt framework was developed to present the rolling information visually and adjust the construction plan in time. The designed processor unit and HCI are shown in Figure 3.

4. Experiments and Discussion

4.1. Positioning Experiments. According to the monitoring requirements and view of highway construction site, the positioning experiments were carried out at a parking lot. The test area was defined rectangular with a length of 15 m and a width of 8 m, where a Cartesian coordinate system was established as shown in Figure 4(a).

The collaborative positioning experiments were carried out based on UWB system and civil GPS system. The UWB base stations were placed at the four vertices of test area, while the x direction and y direction were geographically eastward and northward, respectively. A robotic trolley was selected to travel along a straight line to simulate the rolling movement. At last, the UWB tag and GPS receiver were attached to the trolley together to obtain the positions in real time.

As shown in Figure 4(a), the trolley started at the point (4.5, 0.0), then travelled along the straight line to the end point (9.5, 8.0), and the sampling period T was set as 1 second. Converting GPS message into standard units, the speed was 0.044 m/s and the azimuth was 1.172. The acquired data were processed through extended Kalman filter algorithm, and the results are shown in Figure 4(b).

During the tests, scales were marked along the straight line evenly, a stopwatch was fixed on the trolley, and a handheld camera was used to record the whole moving process. Comparing the real coordinates with positioning coordinates, the errors of typical positions obtained are shown in Figure 4(c). The average accuracy after filtration was 0.48 m, comparing to the usual 10 m.

Based on Figures 4(b) and 4(c), the collaborative positioning system improved the accuracy significantly

Table 1: Typical CCC system products.

Country	Manufacturer	Product	Components
Sweden	Dynapac	DCA system	(1) DGPS/RTK-GPS (Trimble) (2) Industrial computer with CompBase software (3) Acceleration sensor, rear axle sensor, infrared temperature sensor
Germany	BOMAG	AM2 system	(1) DGPS/ATS (Trimble) with BCM 05 software (2) Roller operation control unit (Tablet PC) (3) Acceleration sensor, travel sensor, infrared temperature sensor
Japan	Sakai	CIS2 system	(1) VRS network (Topcon)/MC-R3GPS (2) Operator station (3) Acceleration sensor, infrared temperature sensor
United States	Hammer (Wirtgen Group)	HCQ navigator system	(1) DGPS (Trimble)/OmniStar GPS (2–4 inches) (2) Dashboard with Wi-Fi network (Tablet PC) (3) Acceleration sensor, infrared temperature sensor
United States	Caterpillar	ACC system	(1) MS952 RTK-GPS/SBAS (2) CB460 control box (3) Accelerometer sensor, infrared temperature sensor, pressure sensor, angle sensor
United States	Volvo	Density Direct™ system	(1) DGPS/GPS 3320 radio and receiver (2) Copilot operator station (3) Acceleration sensor, infrared temperature sensor
United States	Case (Amman Group)	ACE system	(1) MS 990 antennas (GPS + GLONASS)/MS972 RTK-GPS (Trimble) (2) CB450 control box (3) Acceleration sensor, slope sensor (AS400), infrared temperature sensor (IS310)

Note. For the protection of intellectual property rights, the CCC systems above are basically installed and used on the rollers of their own manufacturers. DCA, Dynapac Compaction Analyzer; AM2, Asphalt Manager 2; CIS2, Compaction Information System 2; HCQ, Hamm Compaction Quality; ACC, AccuGrade Compaction Control; ACE, Ammann Compaction Expert; ATS, Applicant Tracking System; BCM, BOMAG Compaction Management; RTK, Real-Time Kinematic; SBAS, Satellite-Based Augmentation Systems.

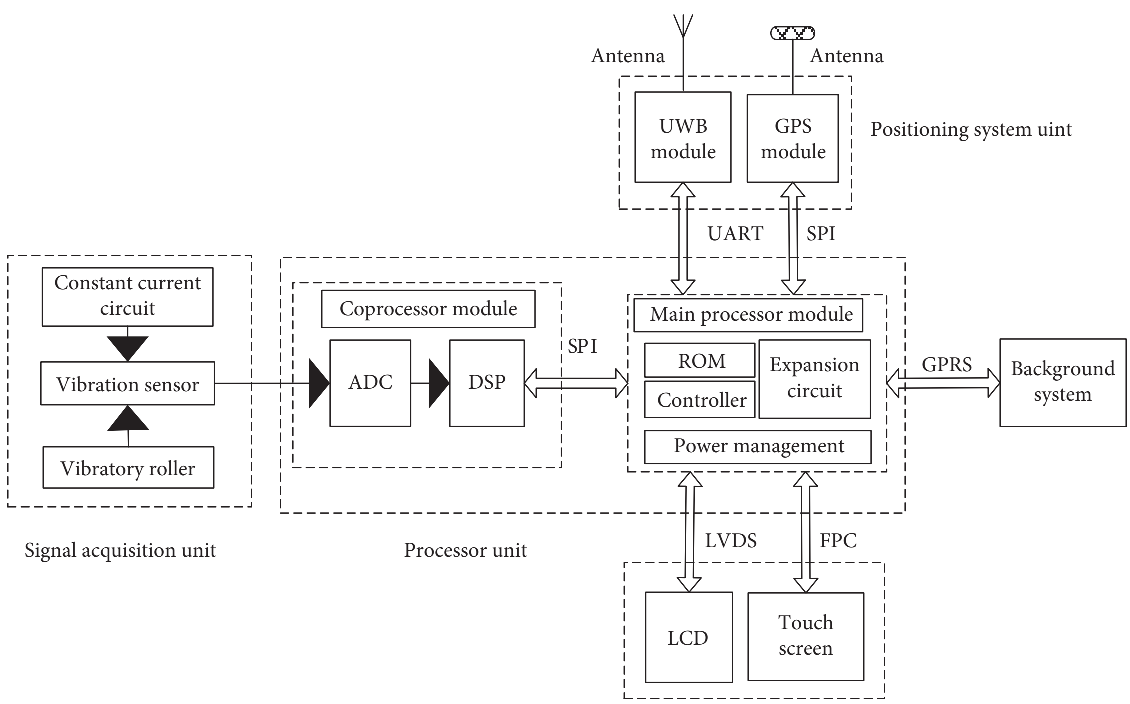

Figure 2: Structure of the compaction detection system. ADC: analog-to-digital converter; DSP: digital signal processing; SPI: serial peripheral interface; UART: universal asynchronous receiver/transmitter; ROM: read-only memory; GPRS: general packet radio service; LVDS: low-voltage differential signaling; FPC: flexible printed circuit; LCD: liquid crystal display.

and corrected the travelling trajectory effectively. Last but not least, the positioning range is not limited to local wireless communication distance. Therefore, the collaborative positioning system based on civil GPS system and UWB system meets the requirements while reducing the cost.

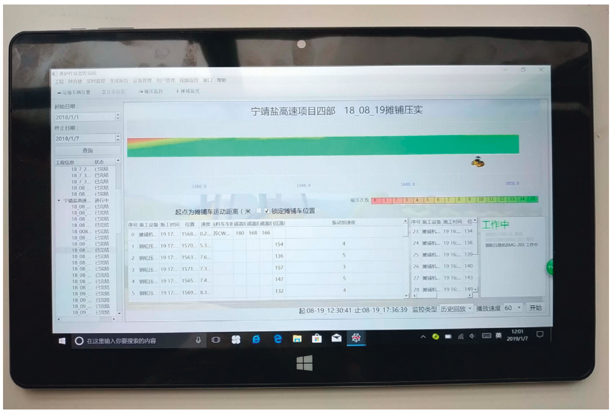

Figure 3: Designed processor unit and HCI.

4.2. Rolling Experiments. The in situ experiments were carried out at the maintenance site of K148 + 12-270 section, S49 highway, China. The thickness of upper layer was 5 cm, and the filling material was SUP20 foam mixed asphalt mixture. According to the rolling process and characteristics, a Cartesian coordinate system was established, while the reference point was set as origin point (0, 0), and the test area was divided as shown in Figure 5.

During the field tests, the average of detected speed was around 1.5 m/s, while the requirement ranges from 5 km/h (1.38 m/s) to 6 km/h (1.67 m/s). The lane width is 3.75 m, and the designed positioning system was mounted on the center of roller roof. Then, it can be considered that the roller travels along the centerline during a single lane rolling pass.

The vibration signals were collected from XD121 roller of XuGong, which worked at 47 Hz. For a segment of original vibration signals, the time-domain waveforms and spectral characteristics are shown as Figures 6(a) and 6(b), respectively.

While the vibratory roller is working, the hydraulic system drives eccentric blocks to rotate at a high speed and then generates forced vibration. During the process, the engine, the frames, etc., introduce complex interferences and noises. In order to reduce the interferences and eliminate the noises, a finite impulse response (FIR) bandpass filter was designed and applied based on Hanning window. The time-domain waveform of the filtered original signal is shown in Figure 6(c), and the smoothness of waveform was improved greatly. The spectral characteristics of the filtered signal are shown in Figure 6(d). The noise of the original signal was suppressed effectively, and the signal-to-noise ratio (SNR) was improved significantly. Therefore, the peaks of fundamental wave as well as the harmonic waves were more obvious than before.

Based on the spectrum image of filtered signal, the amplitude of fundamental wave can be extracted as 3220, the second harmonic wave was 1084, and the third harmonic wave was 183.3. Substituting the amplitudes into equation (4), the CMV value was calculated to be 101. Similarly, multigroup data at 47 Hz frequency were filtered and harmonic extracted, and then CMV, CCV, and VCV_e were calculated with the initial calibration factors.

4.3. Results and Analysis

4.3.1. Compaction of Specific Locations. In order to obtain the compaction quality of asphalt pavement comprehensively, it is necessary to detect the compaction state at specific locations. Taking section 7# as an example, considering the rolling speed, three typical locations, namely, P_1 (2.81, 11.50), P_2 (2.81, 13.00), and P_3 (2.81, 14.50), were selected for analysis as shown in Figure 5. From the time of t_i ($i = 1, 2, 3$ for three rolling pass) on, when roller passed the selected points, the positions and compaction index values were obtained. The results are shown in Table 2, wherein the CMV_1 was the corresponding compaction degree value of first rolling pass, and the others are similar.

Based on Table 2, the following conclusions were made:

(1) Compared with the actual locations of P_1, P_2, and P_3, the positioning errors are within 0.5 m, and the compaction degree values can be obtained with the collaborative positioning system.

(2) Most COV values were less than 15%, indicating that the dispersion of compaction index values at each point was relatively small. Therefore, the compaction degree values were continuous and stable at the selected point substantially. However, some COV values remain larger than 15%. Moreover, these COV values were concentrated in the second pass and became larger on the way from P_1 to P_3 monotonously. Therefore, it can be inferred that the dispersion should not be caused by positioning error. Otherwise, the detection values should be changed randomly with collaborative positioning system. Observing the monitoring video, it is speculated that this phenomenon was related to the roller acceleration in the second pass.

(3) The compaction index values of three measuring points were close to the average of section 7# relatively, indicating that no excessive distortion of the monitoring compaction degree values exists with current positional inaccuracy. Despite this, the difference and dispersion of compaction degree values between three points and section 7# still existed. In the end, the average value cannot represent the compaction degree value of every point, but it still can be used to describe the compaction state of section 7# as a whole.

In summary, with conventional test methods, the roadway can be covered only around one percent. However, the roadway can be covered 100 percent with collaborative positioning system, although its accuracy needs to be improved.

4.3.2. Rolling of Whole Area. To achieve the quality control and quality assurance of construction project, rolling effect of the whole area should be considered. Similarly, the compaction index values in different sections were calculated and the variations of values at different passes are shown in Figures 7(a)–7(c). In addition, the average of

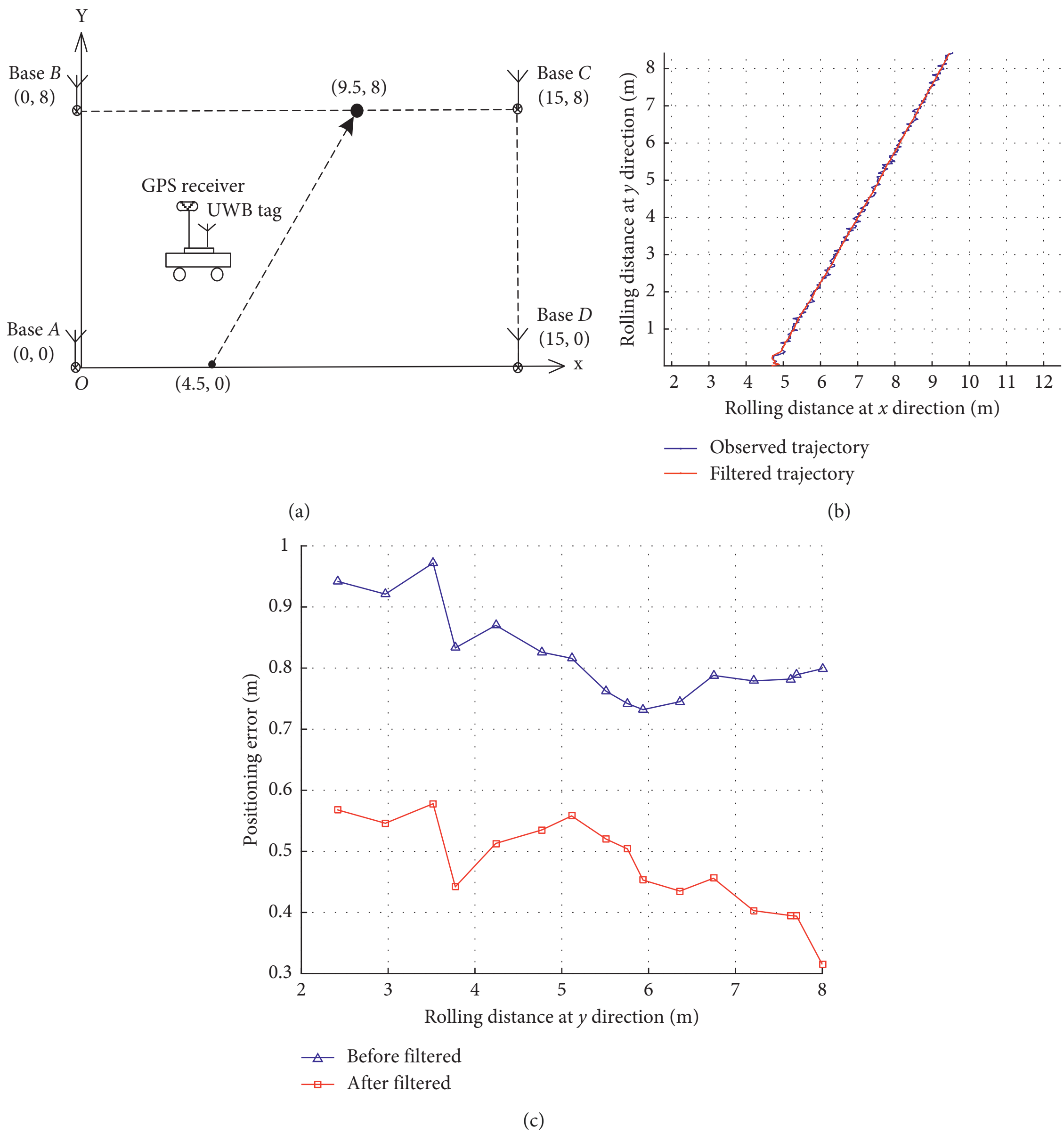

FIGURE 4: Diagram and results of collaborative positioning experiments. (a) Schematic diagram of positioning experiments. (b) Results of positioning experiments. (c) Accuracy analysis of positioning experiments.

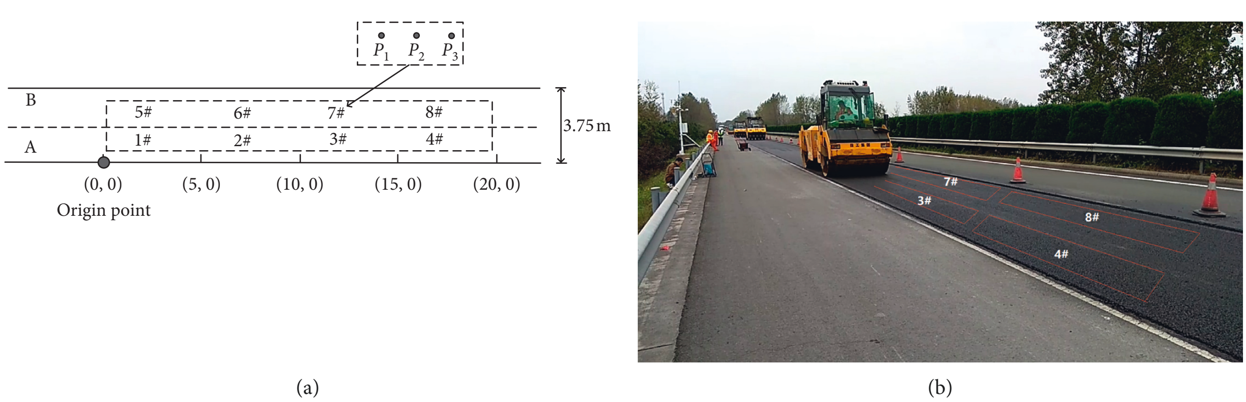

FIGURE 5: Diagram and scene of field rolling experiments. (a) Diagram of in situ rolling experiments. (b) Scene of in situ rolling experiments.

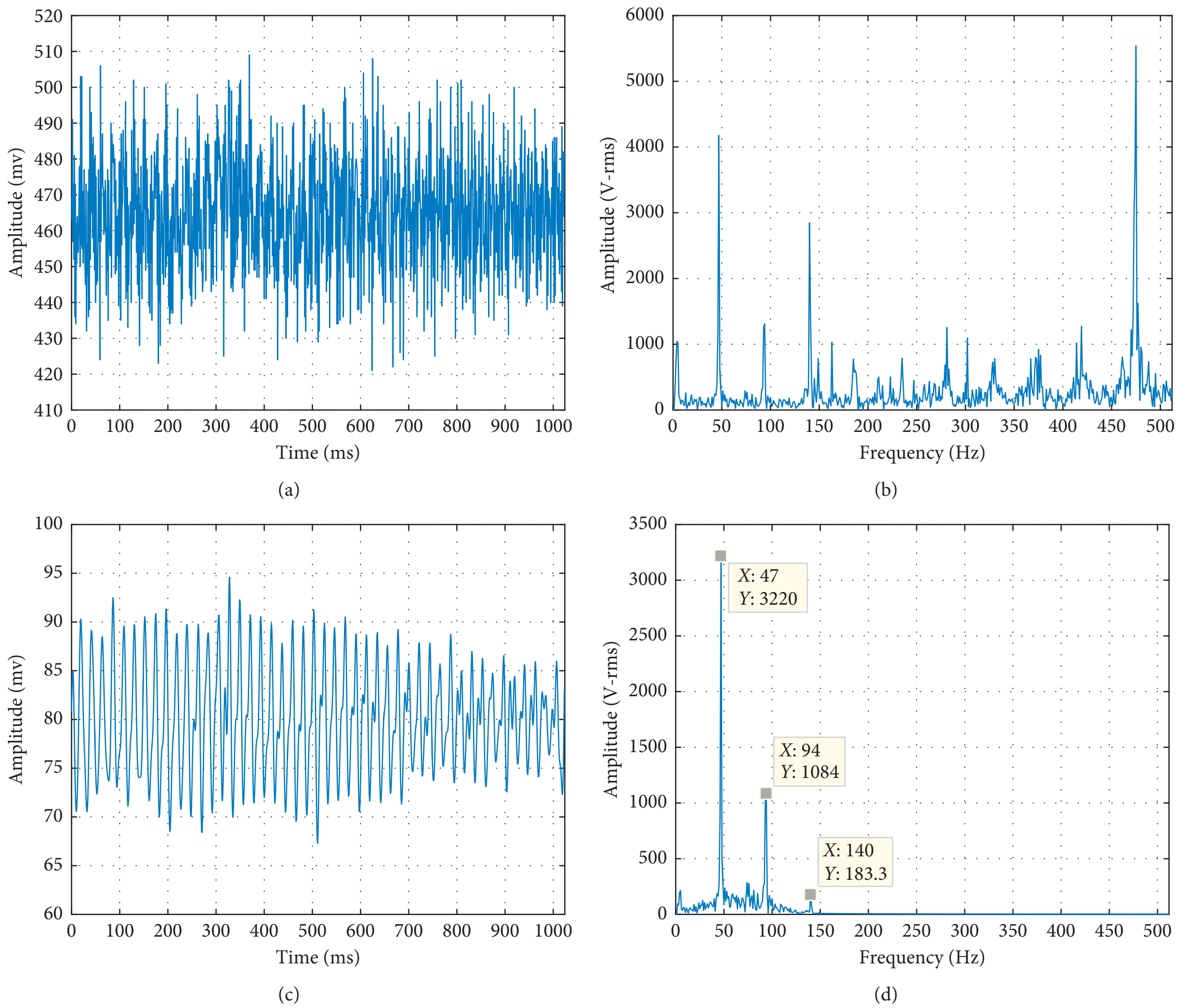

Figure 6: Results of vibration signal processing. (a) Waveforms of the original signal. (b) Frequency waveforms of the original signal. (c) Waveforms of the filtered signal. (d) Frequency waveforms of the filtered signal.

Table 2: Compaction degree results at typical locations of section 7#.

Positioning results	CMV			CCV			VCV_e		
	CMV_1	CMV_2	CMV_3	CCV_1	CCV_2	CCV_3	VCV_{e1}	VCV_{e2}	VCV_{e3}
P_1 (2.97, 11.49)	105.01	84.39	245.27	98.31	101.25	223.18	134.62	59.85	219.59
P_2 (2.93, 13.18)	93.78	145.76	181.74	93.27	168.69	159.54	115.95	127.24	166.50
P_3 (2.99, 14.45)	126.73	206.05	229.71	125.15	240.98	168.49	158.89	178.58	218.74
Average	108.51	145.40	218.91	105.58	170.30	183.74	136.49	121.89	201.61
SD	13.68	49.67	27.04	13.99	57.06	28.13	17.58	48.62	24.83
COV (%)	12.60	34.16	12.35	13.25	33.50	15.31	12.88	39.89	12.32
Average (S7)	107.75	155.93	202.13	109.59	157.79	177.83	103.26	155.95	195.45

SD: standard deviation; COV: coefficient of variation.

referenced compaction degree value was 94.6% by the core sampling method after the final rolling pass. Adjusting the Cal parameters based on the referenced values, the comparison between referenced and calibrated compaction degree values at the final rolling pass is shown as Figure 7(d).

Analysis of the results from whole test area can be concluded as follows:

(1) Comparing the compaction degree values, it is obvious that the values of test sections differ and fluctuate greatly in every rolling pass. By inducting

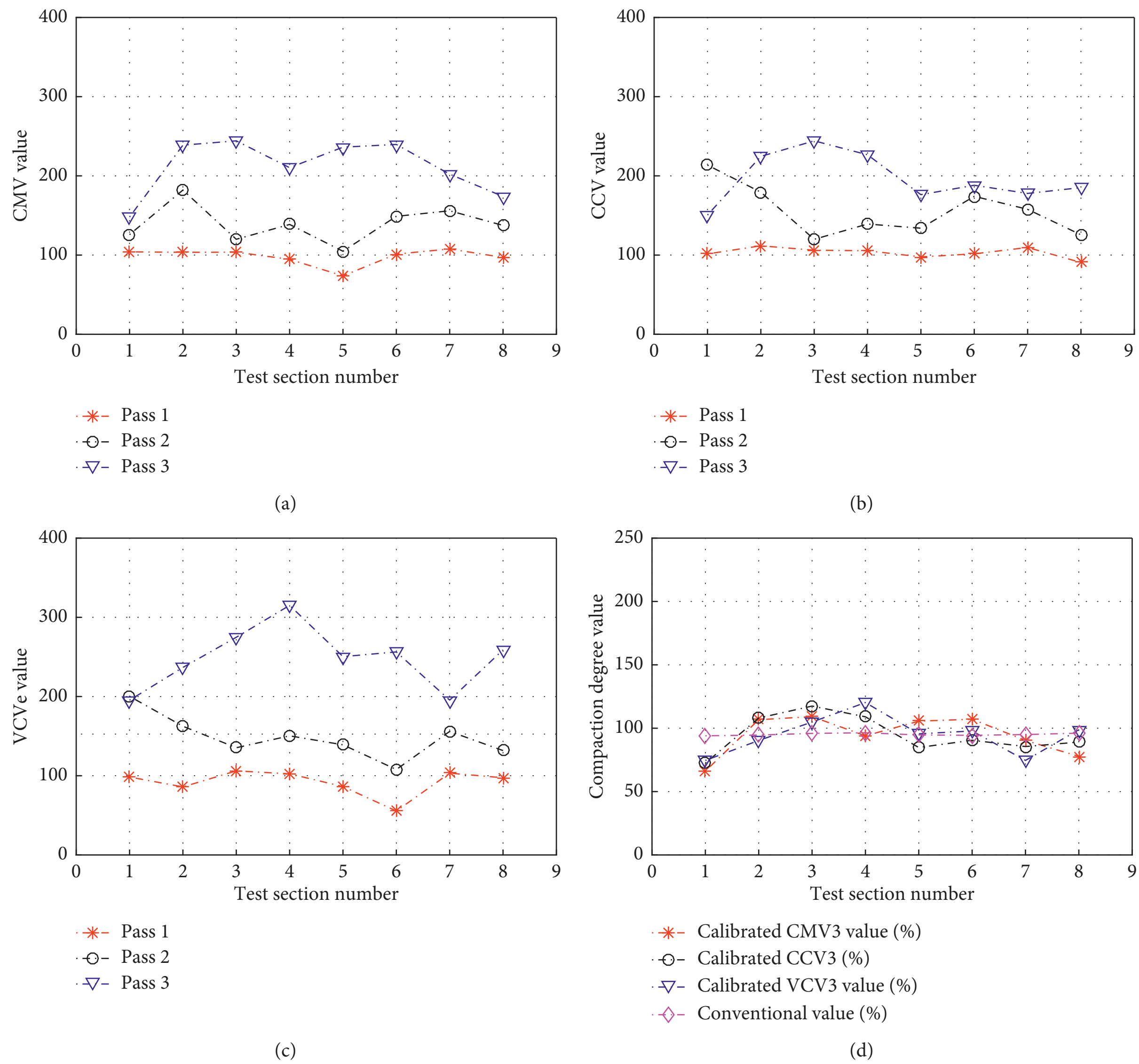

FIGURE 7: Variations of compaction degree values. (a) CMV variation at different rolling passes. (b) CCV variation at different rolling passes. (c) VCV_e variation at different rolling passes. (d) Comparison of compaction values.

the characteristics of abnormal results, it was found that under the same rolling passes, the values varied greatly in section 3# and section 7#. The abnormal changes of all three indexes occur in these sections, thereby eliminating the difference caused by the definition of compaction degree indexes. Reviewing the monitoring video, this phenomenon is closely related to the deceleration, reversing, and lane-changing of roller. This may be attributed to the unstable energy output of roller, resulting in abnormal compaction degree values. On the other hand, the variability of test results can be used to monitor the irregular operations. Based on Figures 4 and 7, it is possible to obtain the rolling effect with positioning data and vibration analysis continuously. Furthermore, CCC system can be realized for the quality evaluation and feedback control.

(2) For the whole test area, as the number of passes increases, it is obvious that the compaction degree of the corresponding test sections increases gradually. The variations of index values are consistent with the rolling process of asphalt mixture. Thus, CMV, CCV, and VCV_e reflect the rolling effects of asphalt pavement to a certain degree. Furthermore, the calculated COV values of CMV, CCV, and VCV_e are 15.61%, 15.08%, and 15.01%. It means that the discrete of VCV_e is less than CMV and CCV. In another way, as an improvement of CMV and CCV, VCV_e is a better index due to the energy perspective and the consideration of as many spectral components as possible.

(3) According to Figure 7(d), the correlation between VCV_e and conventional compaction degree is not strong enough, neither do CMV and CCV. Thereby,

all of them should not be used for quality assurance of pavement compaction directly or alone. Despite this, CMV, CCV, and VCV_e can be used as an auxiliary method for the quality control during rolling process.

5. Conclusions

To detect the compaction degree of asphalt pavement during construction in real time and nondestructively, a low-cost continuous compaction detection method was proposed. A collaborative positioning system based on civil GPS module and UWB module was developed, and the accuracy was improved to 0.48 m, which meets the requirements of rolling positioning. An embedded-based detection system was designed, and dual-processor architecture was proposed to improve the real-time performance and present rolling information, as well as the human-computer interaction. With the responsive vibration signals acquired from the rollers, harmonic analysis was introduced to evaluate the rolling effect. Comparing with the existing compaction degree indexes, a new index VCV_e was proposed in view of the energy distribution. The CMV, CCV, and VCV_e and conventional compaction degree values were obtained in the field experiments separately, and all of them reflect the rolling effects of asphalt pavement to a certain degree. Compared with CMV and CCV, VCV_e is less discrete, more stable, and consistent to describe the compaction effect. Though all the CMV, CCV, and VCV_e indexes possess limitations and cannot be the criterion for quality assurance, the level of compaction can still be indicated in general and thus serve as a reference for quality control. In summary, with the application of collaborative positioning system, online detecting technology, and monitoring software, the continuous compaction detection method could meet the monitoring requirements of asphalt pavement during compaction at a lower cost and lay a foundation for the intelligent compaction.

Data Availability

The data used to support the findings of this study are included within the article.

Conflicts of Interest

The authors declare that there are no conflicts of interest regarding the publication of this paper.

Acknowledgments

This research was supported by the National Natural Science Foundation of China (grant no. 51678146) and the Postgraduate Research and Practice Innovation Program of Jiangsu Province (grant no. KYCX_0169). The authors gratefully acknowledge their financial support. The authors would like to acknowledge all those who participated in the field tests at the highway maintenance site. Additionally, all the authors of the following references are much appreciated.

References

[1] N. Tran, T. Pamela, and S. James, *Enhanced Compaction to Improve Durability and Extend Pavement Service Life: A Literature Review*, National Center for Asphalt Technology, Auburn, AL, USA, 2016.

[2] J. Li, G. Liu, T. Yang, J. Zhou, and Y. Zhao, "Research on relationships among different distress types of asphalt pavements with semi-rigid bases in China using association rule mining: a statistical point of view," *Advances in Civil Engineering*, vol. 2019, Article ID 5369532, 15 pages, 2019.

[3] B. C. Smith and B. K. Diefenderfer, "Comparison of nuclear and nonnuclear pavement density testing devices," *Transportation Research Record: Journal of the Transportation Research Board*, vol. 2081, no. 1, pp. 121–129, 2008.

[4] S. Cui, X. Wang, and F. Zhou, "Development of real-time compaction detection and intelligent compaction technology," *Journal of Road Machinery & Construction Mechanization*, vol. 3, pp. 18–22, 2013.

[5] J. Li, M. Shang, G. Liu et al., "Two-step improvements of volumetric design method based on multi-point supported skeleton for asphalt mixtures," *Construction and Building Materials*, vol. 217, pp. 456–472, 2019.

[6] Y. K. Wu, H. Y. Wang, and X. S. Sang, "The research on testing processing effect of dynamic compaction subgrade based on transient Rayleigh wave method," *Applied Mechanics and Materials*, vol. 357–360, pp. 1531–1534, 2013.

[7] J. L. Chai and Y. Wang, "The application research of non-nuclear density gauge electromagnetic technology in the road engineering," *Applied Mechanics and Materials*, vol. 597, pp. 384–387, 2014.

[8] B. Umashankar, C. Hariprasad, and G. T. Kumar, "Compaction quality control of pavement layers using LWD," *Journal of Materials in Civil Engineering*, vol. 28, no. 2, article 4015111, 2015.

[9] F. Beainy, S. Commuri, and M. Zaman, "Quality assurance of hot mix asphalt pavements using the intelligent asphalt compaction analyzer," *Journal of Construction Engineering and Management*, vol. 138, no. 2, pp. 178–187, 2012.

[10] C. L. Meehan, D. V. Cacciola, F. S. Tehrani, and W. J. Baker, "Assessing soil compaction using continuous compaction control and location-specific in situ tests," *Automation in Construction*, vol. 73, pp. 31–44, 2017.

[11] C. M. Savan, K. W. Ng, and K. Ksaibati, "Benefit-cost analysis and application of intelligent compaction for transportation," *Transportation Geotechnics*, vol. 9, pp. 57–68, 2016.

[12] M. Barman, M. Nazari, S. A. Imran et al., "Quality control of subgrade soil using intelligent compaction," *Innovative Infrastructure Solutions*, vol. 1, no. 1, pp. 1–14, 2016.

[13] D. Liu, M. Lin, and S. Li, "Real-time quality monitoring and control of highway compaction," *Automation in Construction*, vol. 62, pp. 114–123, 2016.

[14] T. Kim and S. Ryu, "Intelligent compaction terminal system for asphalt pavement in korea," *Journal of Emerging Trends in Computing and Information Sciences*, vol. 6, no. 3, pp. 154–158, 2015.

[15] J. Oh, "A review on intelligent compaction techniques in railroad construction," *International Journal of Railway*, vol. 7, no. 3, pp. 80–84, 2014.

[16] D. Liu, Z. Li, and Z. Lian, "Compaction quality assessment of earth-rock dam materials using roller-integrated compaction monitoring technology," *Automation in Construction*, vol. 44, pp. 234–246, 2014.

[17] P. Erdmann and D. Adam, "Numerical simulation of dynamic soil compaction with vibratory compaction equipment," in *Proceedings of the XV Danube—European Conference on Geotechnical Engineering (DECGE 2014)*, pp. 243–248, Wien, Austria, September 2014.

[18] C. Herrera and B. Caicedo, "Finite difference time domain simulations of dynamic response of thin multilayer soil in continuous compaction control," *Procedia Engineering*, vol. 143, pp. 411–418, 2016.

[19] H. F. Thurner, "Method and a device for ascertaining the degree of compaction of a bed of material with a vibratory compacting device," *Journal of the Acoustical Society of America*, vol. 65, no. 5, pp. 1356-1357, 1979.

[20] K. Anjan, R. Aldouri, S. Nazarian, and J. Si, "Accelerated assessment of quality of compacted geomaterials with intelligent compaction technology," *Journal of Construction and Building Materials*, vol. 113, pp. 824–834, 2016.

[21] D. J. White and M. J. Thompson, "Relationships between in situ and roller-integrated compaction measurements for granular soils," *Journal of Geotechnical and Geoenvironmental Engineering*, vol. 134, no. 12, pp. 1763–1770, 2008.

[22] Q. Xu, G. K. Chang, and V. L. Gallivan, "A sensing-information-statistics integrated model to predict asphalt material density with intelligent compaction system," *IEEE/ASME Transactions on Mechatronics*, vol. 20, no. 6, pp. 3204–3211, 2015.

[23] D. V. Cacciola, C. L. Meehan, and M. Khosravi, "An evaluation of specification methodologies for use with continuous compaction control equipment," in *Proceedings of the International Conference of Geo-Congress*, pp. 413–416, Reston, VA, USA, March 2013.

[24] P. Dou, Z. Nie, and X. Wang, "Correlation verification of railway subgrade compaction quality test value between CMV and Evd," *Journal of Railway Science and Engineering*, vol. 11, no. 2, pp. 90–94, 2014.

[25] Federal Highway Administration, "Intelligent compaction measurement values (ICMV)—a road map," Federal Highway Administration, Washington, DC, USA, 2017, http://www.fhwa.dot.gov/construction/ictssc/pubs/hif17046.pdf.

[26] G. Xu, H. Gao, Z. Luo, J. Huang, and D. Wang, "Application of continuous and intelligent compaction control technology in high-speed railway construction application of continuous and intelligent compaction control technology in high-speed railway construction," *Journal of Railway Science and Engineering*, vol. 1, pp. 30–34, 2017.

[27] K. Kim, *Numerical Simulation of Impact Rollers for Estimating the Influence Depth of Soil Compaction*, Master thesis, Texas A & M University, College Station, TX, USA, 2010.

[28] Y. Gao, X. Huang, and W. Yu, "The compaction characteristics of hot mixed asphalt mixtures," *Journal of Wuhan University of Technology-Mater. Sci. Ed.* vol. 29, no. 5, pp. 956–959, 2014.

[29] Federal Highway Administration, "Intelligent compaction knowledge base, workshops, projects, support, specifications," Federal Highway Administration, Washington, DC, USA, 2018, https://www.fhwa.dot.gov/pavement/ic/.

[30] M. E. Abdullah, K. Ahmad Zamhari, R. Buhari et al., "Warm mix asphalt technology: a review," *Jurnal Teknologi*, vol. 71, no. 3, pp. 39–52, 2014.

[31] P. Manuel, C. Jacob, A. Juan, and R. Antonio, "Development and evaluation of a combined cultivator and band sprayer with a row-centering RTK-GPS guidance system," *Sensors*, vol. 13, no. 3, pp. 3313–3330, 2013.

[32] Q. Xu, G. K. Chang, and V. L. Gallivan, "Development of a systematic method for intelligent compaction data analysis and management," *Construction and Building Materials*, vol. 37, pp. 470–480, 2012.

[33] X. Zhang, L. Wei, D. Cao, L. Zhao, and M. Jin, "Research on applicability of intelligent compaction for asphalt pavement," *Journal of China Foreign Highhway*, vol. 6, pp. 69–73, 2016.

[34] Z. Nie, X. Wang, and T. Jiao, "Anomalous data detection for roller-integrated compaction measurement," *International Journal of Geomechanics*, vol. 16, no. 1, article B4015004, 2015.

[35] N. I. C. Z. Barman, "Application of intelligent compaction technique in real time evaluation of compaction level during the construction of subgrade," in *Proceedings of the 93th Transportation Research Board Annual Meeting*, Washington, DC, USA, January 2014.

[36] D. Singh, F. Beainy, S. Commuri, and M. Zaman, "Application of intelligent compaction technology for estimation of an effective modulus for a multilayered asphalt pavement," in *Proceedings of the International Conference on Sustainable Civil Infrastructure (Geo-Hubei)*, pp. 51–58, American Society of Civil Engineers, Wuhan, Hubei, China, July 2014.

[37] Q. Xu and G. K. Chang, "Adaptive quality control and acceptance of pavement material density for intelligent road construction," *Automation in Construction*, vol. 62, pp. 78–88, 2016.

[38] N. S. Matharu and A. S. Buttar, "An efficient approach for localization using trilateration algorithm based on received signal strength in wireless sensor network," *International Journal of Computer Science and Information Security*, vol. 3, pp. 11–16, 2016.

[39] A. Vasenev, *Visualizing Asphalt Roller Trajectories in Context: Acquiring, Processing, and Representing Sensor Readings*, Doctor dissertation, Universiteit Twente, Enscheda, Overijsse, Netherlands, 2015.

[40] Z. Li, G. Chang, J. Gao, J. Wang, and A. Hernandez, "GPS/UWB/MEMS-IMU tightly coupled navigation with improved robust Kalman filter," *Advances in Space Research*, vol. 58, no. 11, pp. 2424–2434, 2016.

[41] B. Kenneally, O. M. Musimbi, J. Wang, and M. A. Mooney, "Finite element analysis of vibratory roller response on layered soil systems," *Computers and Geotechnics*, vol. 67, pp. 73–82, 2015.

[42] A. V. Oppenheim, A. S. Willsky, and S. H. Nawab, *Signals & Systems*, Prentice-Hall, Upper Saddle River, NJ, USA, 2nd edition, 1996.

[43] J. W. Cooley and J. W. Tukey, "An algorithm for the machine calculation of complex fourier series," *Mathematics of Computation*, vol. 19, no. 90, pp. 297–301, 1965.

[44] F. Beainy, S. Commuri, and M. Zaman, "Dynamical response of vibratory rollers during the compaction of asphalt pavements," *Journal of Engineering Mechanics*, vol. 140, no. 7, article 04014039, 2014.

[45] T. Hua, X. Yang, Q. Yao, and H. Li, "Assessment of real-time compaction quality test indexes for rockfill material based on roller vibratory acceleration analysis," *Advances in Materials Science and Engineering*, vol. 2018, Article ID 2879321, 15 pages, 2018.

[46] Federal Highway Administration, "Techbrief: intelligent compaction," Federal Highway Administration, Washington, DC, USA, 2018, http://www.fhwa.dot.gov/construction/pubs/hif13051.pdf.


Journal of Engineering
The Scientific World Journal
International Journal of Rotating Machinery
Journal of Sensors
Advances in Multimedia
Advances in Civil Engineering
Hindawi
Submit your manuscripts at
www.hindawi.com
Journal of Control Science and Engineering
Journal of Robotics
Journal of Electrical and Computer Engineering
Advances in OptoElectronics
VLSI Design
International Journal of Navigation and Observation
Modelling & Simulation in Engineering
International Journal of Aerospace Engineering
International Journal of Chemical Engineering
International Journal of Antennas and Propagation
Active and Passive Electronic Components
Shock and Vibration
Advances in Acoustics and Vibration